

Stability of plasma-treated silicone rubber and its influence on the interfacial aspects of blood compatibility

R.L. Williams^{a,*}, D.J. Wilson^{a,1}, N.P. Rhodes^{a,b}

^a *Department of Clinical Engineering, University of Liverpool, Duncan Building, Daulby Street, Liverpool L69 3GA, UK*

^b *UK Centre for Tissue Engineering, University of Liverpool, Daulby Street, Liverpool L69 3GA, UK*

Received 25 June 2003; accepted 4 December 2003

Abstract

Medical-grade polydimethylsiloxane elastomer was subjected to low-powered plasma treatment in the presence of four different gases: O₂, Ar, N₂ and NH₃. Changes to the surface chemistry immediately after processing and the stability of the treatments following ageing in phosphate buffered saline or air for up to 1 month were investigated using X-ray photoelectron spectroscopy and dynamic contact angle analysis. Changes in surface morphology were assessed using optical microscopy and atomic force microscopy. All treatments resulted in an increase in wettability, attributed to major changes in chemistry combined with modest etching. Furthermore, the primary site of attack of the plasma species appeared to be dependent upon the feed gas implemented. The two main chemical changes observed after ageing were due to reactions with the storage media and relaxation processes resulting in further changes in wettability. The influence of the surface modifications on the blood compatibility of the materials was investigated by assessing contact phase activation using a partial thromboplastin time assay. It was demonstrated that the O₂ and Ar plasma treatments reduced the performance of the silicone but the N₂ and NH₃ treatments had a significantly beneficial effect on the activation of the coagulation cascade.

© 2003 Elsevier Ltd. All rights reserved.

Keywords: Silicone; Surface modification; Gas plasma; Blood compatibility; Coagulation

1. Introduction

Silicone rubber has been widely used in medical devices, in particular, those in contact with blood and the vasculature due to its specific mechanical properties (compliance, softness) and relatively good blood compatibility. Nevertheless, many studies have indicated that blood contact with silicone can lead to the formation of thrombi and emboli [1,2] and so in low-shear environments its use is generally limited to short-term blood contact. Plasma modification of silicone rubber has previously been extensively researched [3–15]. Various gases have been used in the modification process to treat these surfaces, such as O₂ [3,4], NH₃ [5], N₂ [4,5] and Ar [4–6] and the use of plasmas with different excitation frequencies is often responsible for

some of the major differences observed. Usually, a multiplicity of species can be obtained, e.g. inorganic silica [4,10,11] and oxidised carbon species such as carbonyl and aldehydes [5,6] which results in a significant increase in surface wettability [9]. An additional observation is the nucleation of small microcracks which form as a result of the brittle nature of the modified surfaces [4]. The precise modifications produced are dependent on the characteristics of the particular plasma created in the system used [16,17]. This can make it difficult to compare the results of one study with another when they use a different plasma system; it is therefore critically important to assess the surface properties created in each case.

The interaction of biomaterials with any biological fluid is largely controlled by the adsorbed protein layer. The major reactions and cellular interactions that occur as a result of this adsorption from blood are due to conformational changes relative to the native, soluble form of the protein molecules and their orientation. Since protein molecules, as a generic group, are only sparingly soluble, the material–protein interaction is

*Corresponding author. Tel.: +44-151-7064205; fax: +44-151-7065803.

E-mail address: rlw@liverpool.ac.uk (R.L. Williams).

¹ Current address: Smith and Nephew Group Research Centre, York Science Park, York Y10 5DF, USA.

controlled by the surface wettability and chemistry, since proteins will attempt to minimise their energy state by forming hydrophobic interactions. Even small changes in surface energy, therefore, can have a dramatic change in the biological response to the surface by virtue of the complex nature of the conformation and orientation of the adsorbed proteins.

Although there is a controlling effect of the surface chemistry and wettability on biomaterial thrombogenicity [18,19], no direct or linear relationship between the two has been demonstrated [20]. Indeed, there has been a long desire to correlate biomaterial characteristics with biological performance [21], including surface energy and tension [22–24] and surface charge [25], but with no obvious success, both subtle and sometimes large differences giving rise to unremarkable changes in biocompatibility [26,27]. The purpose of the current study was to investigate whether it was possible to modify the interfacial reactions related to the blood contact properties of a commonly used biomaterial using only a simple chemical change, and investigate the extent of those surface chemical alterations.

The stability of plasma-treated polymers in various ageing environments has been the subject of many investigations often demonstrating that the surface modifications are transient [15]. In the context of biomedical devices, it is important to establish the ageing characteristics of materials during the period from plasma treatment to implantation, and post-implantation. Thus, the objective of this investigation was not only to report on the surface modification of polydimethylsiloxane (PDMS) by O₂, Ar, N₂ and NH₃ plasmas immediately after processing, but also after ageing in either phosphate buffered saline (PBS) or air for time periods up to 1 month. All materials were characterised in detail using the following complementary techniques: X-ray photoelectron spectroscopy (XPS); atomic force microscopy (AFM); scanning electron microscopy (SEM) and dynamic contact angle (DCA) measurements both immediately after treatment and following ageing to determine changes in surface chemistry, roughness and wettability.

The major effect of blood–biomaterial contact on protein systems is the activation of the coagulation and complement cascades. The effect of the surface modifications on the interfacial reactions, therefore, was extrapolated from the influence of the surfaces on the acellular component of blood, platelet poor plasma (PPP), using a partial thromboplastin time (PTT) assay.

2. Materials and methods

2.1. Materials

Medical-grade PDMS elastomer was purchased in sheet form (2 mm thick) from A Littlejohn Ltd. (type

MED-4050, Cowbridge, UK). This grade of material contained fillers and vulcanising agents, but did not contain other additives which are normally used in organic rubber compounding. The PDMS was cut into rectangular pieces (10 × 20 mm) for physico-chemical experiments and circular coupons 25 mm in diameter for biological analysis, which were cleaned using diethyl ether to remove surface contaminants and low molecular weight species prior to plasma treatment. All samples were handled thereafter with surgical gloves and tweezers to minimise contamination. Four ultra-purity-grade reactor gases: O₂: 99.5%; Ar: 99.998%; N₂: 99.998%; NH₃: 99.99% were purchased from BOC Ltd. (Guildford, Surrey, UK) and were used as supplied.

2.2. Plasma treatment

The radiofrequency (RF) equipment and treatment procedure used in this study has been outlined in detail previously [28,29]. Briefly, a low-powered plasma was produced in a half-wave helical resonator formed from a 100-turn copper wire wound directly on the outside of a glass tube. The excitation frequency and RF power was 13.6 MHz and <1 W, respectively [30]. In all experiments, treatment time was 1 min, the gas pressure set at 8×10^{-2} mbar and the flow rate 85 sccm. The gas species admitted to the reactor (O₂, Ar, N₂ and NH₃) was the only experimental variable during sample treatment.

2.3. Ageing procedure

Materials were stored in plastic vials containing air or PBS at 37°C and examined after time periods of 20 min, 2, 6, 24 h, 1 week and 1 month. Untreated specimens underwent the same ageing procedure for comparison. Samples aged in air were wrapped in aluminium foil to minimise hydrocarbon contamination. Samples aged in PBS were thoroughly washed in deionised water and then dried using pressurised air before analysis.

2.4. X-ray photoelectron spectroscopy (XPS)

The equipment and procedure has been described in detail elsewhere [16,17]. Briefly, XPS was carried out using a VG Scientific ESCALAB MXII spectrometer (East Grinstead, UK) using an unmonochromated AlK α radiation for excitation of the sample and operated at 12 kV and 240 W. Angle resolved work was carried out on selective samples at take-off angles ranging from 15° to 70°. High-resolution spectra were examined in the sequence: C-1s, Si-2p, O-1s, N-1s and C-1s. Repeating the C-1s ensured that the surface had not been subjected to excess radiation damage. Charging of the surface was not controlled since no flood gun/screen technique was available. Therefore, the C-1s component due to carbon

involved in siloxane (C–Si–O–Si) (284.7 eV) in the C-1s spectrum for control and treated surfaces was used as a binding energy reference for all spectra collected [12]. Atomic composition data were carried out using empirical sensitivity factors and all experimental peaks were integrated after non-linear background subtraction using the software provided.

2.5. Microscopy

The surface topography of virgin- and plasma-treated specimens was examined by optical microscopy and AFM using a Digital Instruments Nanoscope III AFM (Santa Barbara, CA, USA). AFM operated in ‘tapping mode’ was used to determine changes in microroughness induced by plasma treatment. The root mean squared (RMS) roughness and relative surface area, a_r , compared to a flat surface, were subsequently determined on at least five independent areas of a surface.

2.6. Contact angle measurements

DCA measurements were performed on untreated and plasma-treated materials by the Wilhelmy plate technique using a computer-controlled Cahn Instruments DCA322 dynamic contact analyser (Manchester, UK). Mean values of advancing and receding angles (θ_A and θ_R , respectively) were determined by averaging the measurements obtained from cycles carried out on at least five independent specimens of both untreated and treated surfaces. All DCA measurements were performed using PBS, made up to pH 7.4 with the following composition: 0.01 M phosphate buffer (80% NaH_2PO_4 and 20% Na_2HPO_4), 0.27 mM KCl and 0.137 M NaCl in distilled water.

2.7. Preparation of platelet poor plasma (PPP)

Blood was collected from a median cubital vein of healthy male volunteers who had not taken medication for at least 14 days and anticoagulated by the addition of 3.8% (w/v) tri-sodium citrate at a volume ratio of 1 citrate to 9 blood. The occurrence of thromboplastic species was reduced by performing phlebotomy without the use of a tourniquet. A high-purity PPP pool was generated from several volunteers by removing from each sample most of the blood cells using conventional means (centrifugation at 250g, 10 min) then respinning at 13 000g for 30 s in a microcentrifuge. The consistency of the pool was ensured by rapidly snap-freezing 250 μl aliquots of the plasma pool in liquid nitrogen, then storing until use at -80°C . Plasma aliquots were used in the analysis of contact phase activation after prewarming the frozen tubes for 60 s at 37°C in a water bath.

2.8. Contact phase activation measurements

Activation of the coagulation system (contact phase activation) after incubation of PPP with untreated and plasma-treated specimens was determined by PTT analysis, as described previously [30]. The clotting times of plasma aliquots were measured using an Instrumentation Laboratory ACL300 Research coagulometer (Milan, Italy). Disc shaped samples (25 mm diameter) were placed into 6-well plates and incubated with 200 μl of PPP at 37°C for 10 min, such that the whole sample surface was covered but *not contacting* the 6-well plate. The relative humidity in the incubator was maintained at $\geq 95\%$ to prevent PPP evaporation. After 10 min incubation, 80 μl of PPP was removed from each sample and added to coagulometer sample vials. Systematic error in the estimation of activation due to differential contact time was prevented by removing PPP from samples in the same order as addition. During the automated analysis of contact phase activation, an equal volume of CaCl_2 (25 mM) and platelet substitute (partial thromboplastin) (Diagen reagent, Diagnostic Reagents Ltd., Thame, Oxfordshire, UK) was added to the PPP samples, which were maintained at 37°C within the coagulometer. The activation status of each set of materials was analysed simultaneously to prevent systematic error (temperature variation, etc.). Each sample was measured spectrophotometrically 10 times/s for 400 s. The coagulometer initiates the clotting reaction by the addition of CaCl_2 , the progress of the reaction monitored by measuring the turbidity against an optical reference. Unfiltered clotting curves of light transmittance vs. time were exported to a computer and the clotting times determined from this graph; the clotting time was defined as the time taken for the turbidity to reach the 3% threshold value (97% transmittance) compared with an unclotted baseline and the optical reference. Uncontacted PPP- and kaolin-treated plasma were used as negative and positive controls, respectively; the kaolin (Sigma, Poole, Dorset, UK) was used as a stock suspension of 1 g/l in barbitone buffer (24 mM 5,5-diethylbarbituric acid, 73 mM tris-(hydroxymethyl) aminomethane, 0.79 M calcium lactate, 2.5 mM sodium azide, pH 7.4). In this case, 65 μl of plasma was incubated with 35 μl of kaolin for 10 min, and this solution used in the coagulometer to assess clotting time.

2.9. Statistics

The results of the PTT assays were analysed by ANOVA, corrected using a Bonferroni procedure and tested for data interaction using a Tukey test, with $n = 4$ for each plasma treatment.

3. Results

3.1. X-ray photoelectron spectroscopy (XPS)

Elemental ratios for the different plasma treatments are shown in Figs. 1–4 and the relative integrated peak areas for the major corrected binding energies of deconvoluted peaks for C-1s, Si-2p, O-2s and N-s2 are listed in Tables 1 and 2. Chemical assignments for deconvoluted peaks were based on binding energies quoted in the literature [31]. The uncertainty in relative area quoted for each deconvoluted peak is approximately 10%, i.e. comparable with experimental errors for the XPS techniques.

3.1.1. Untreated material

Initial elemental analysis of untreated silicone rubber indicated no surface contamination; a Si:O:C ratio of

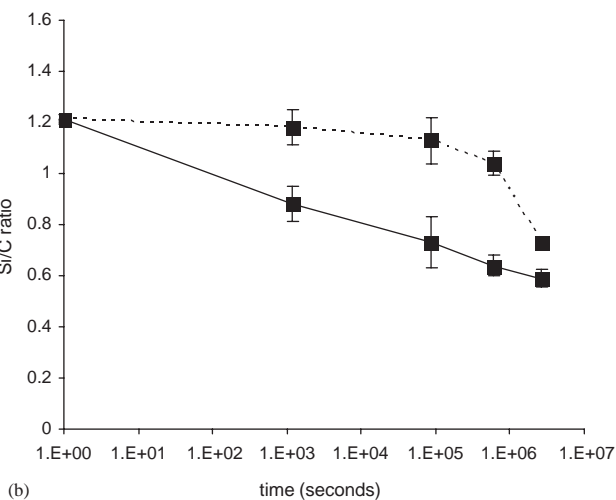
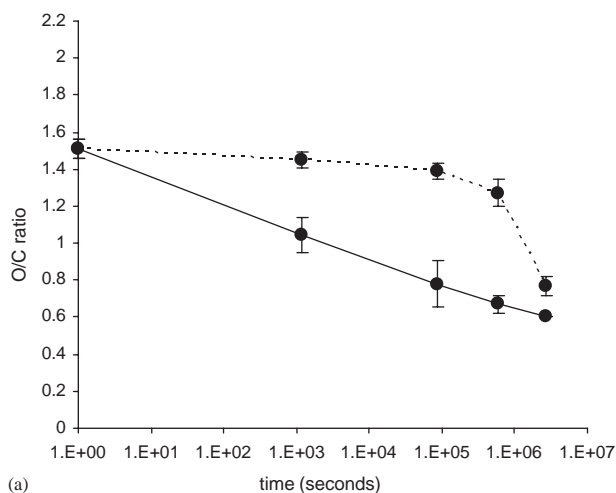


Fig. 1. Elemental ratios of O₂ plasma-treated PDMS as a function of time; (a) O/C; and (b) Si/C. (—) Storage in PBS; and (---) storage in air. Mean \pm standard deviation, $n = 3$.

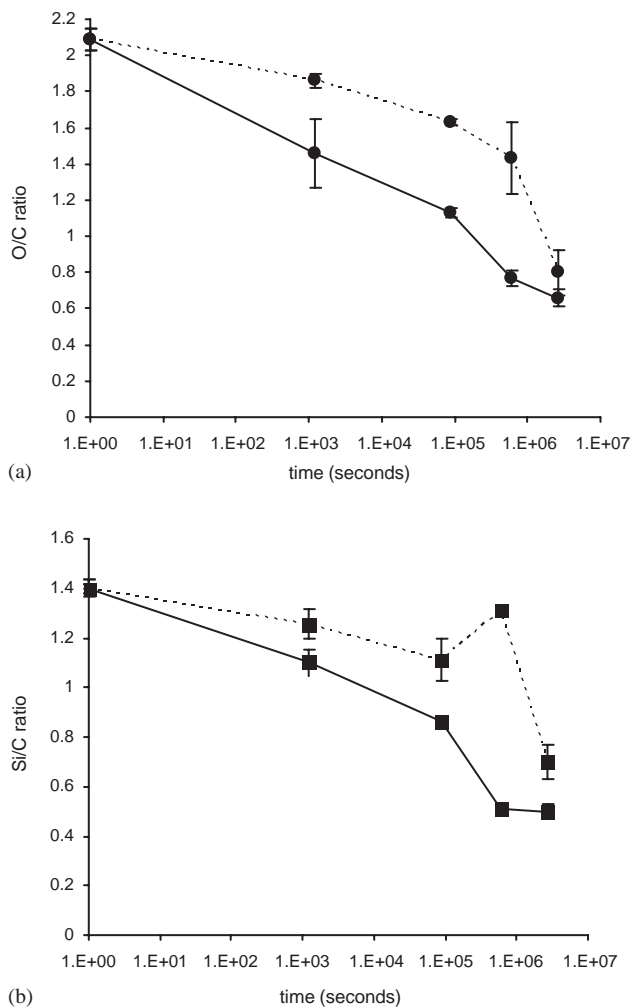
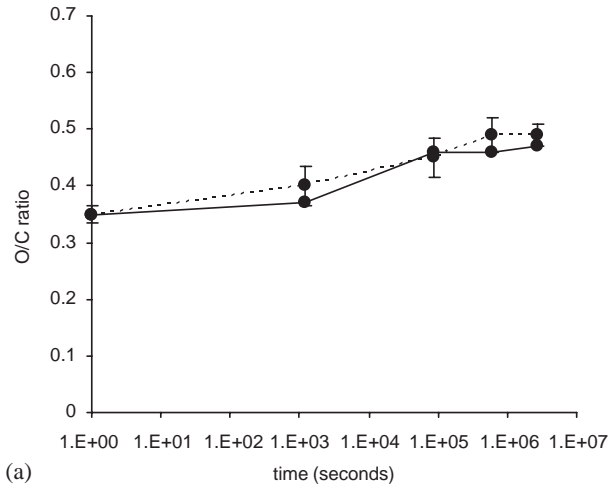
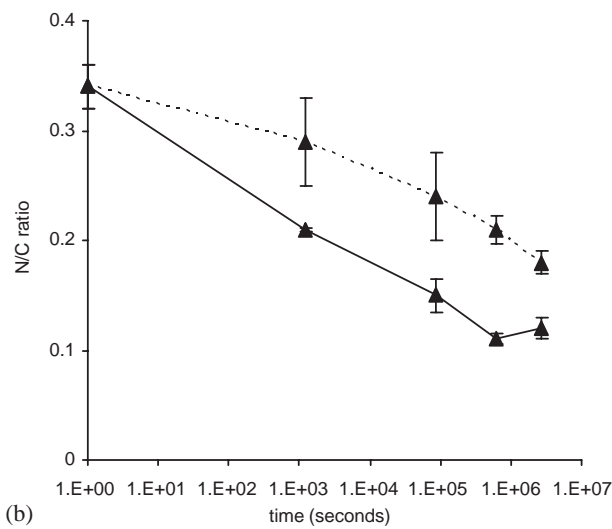


Fig. 2. Elemental ratios of Ar plasma-treated PDMS as a function of time; (a) O/C; and (b) Si/C. (—) Storage in PBS; and (---) storage in air. Mean \pm standard deviation, $n = 3$.

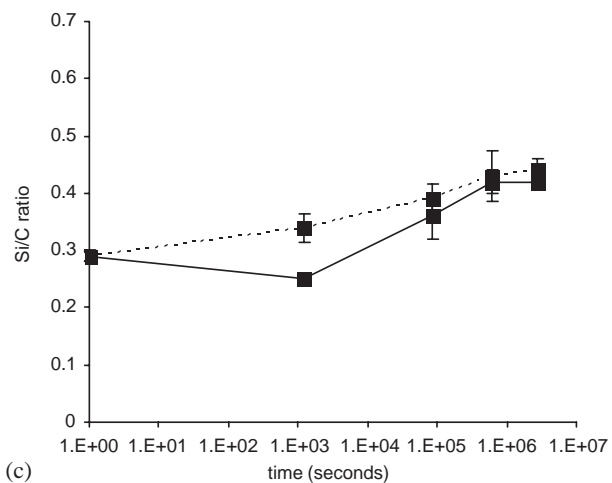
approximately 1:1:2 was found which is anticipated for this material. Furthermore, no variation in composition was observed with sample depth. The high-resolution C-1s spectrum was symmetrical (full width at half maximum (FWHM) of 1.5 eV) indicative of (C–Si–O–Si) bonds [12]. The Si-2p spectrum (FWHM 1.8 eV) centered at 102.2 eV was deconvoluted into two components. The most intense peak was assigned to –O–Si–O–R₂– bonds (102.4 eV) indicative of a polysiloxane structure. A less intense component at higher binding energy was also observed, 103.6 eV, characteristic of silica filler. The O-1s spectrum was also sharp (FWHM 1.7 eV) and symmetrical and could be deconvoluted into one species (532.4 eV) assigned to O–Si–O. Ageing in PBS for periods of up to 1 month did not result in any appreciable change in the elemental composition of untreated materials, confirming the inert nature of PDMS.



(a)



(b)

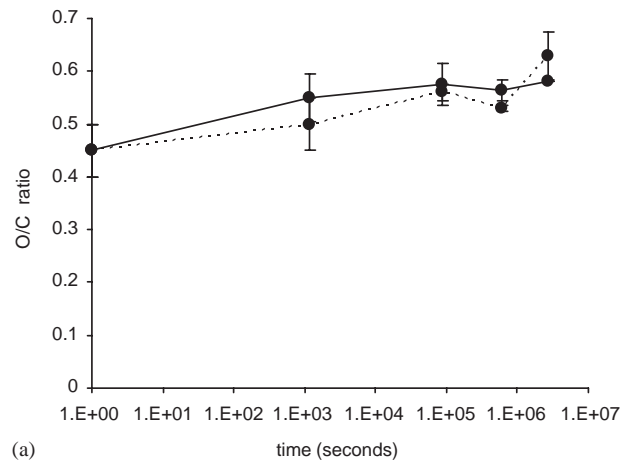


(c)

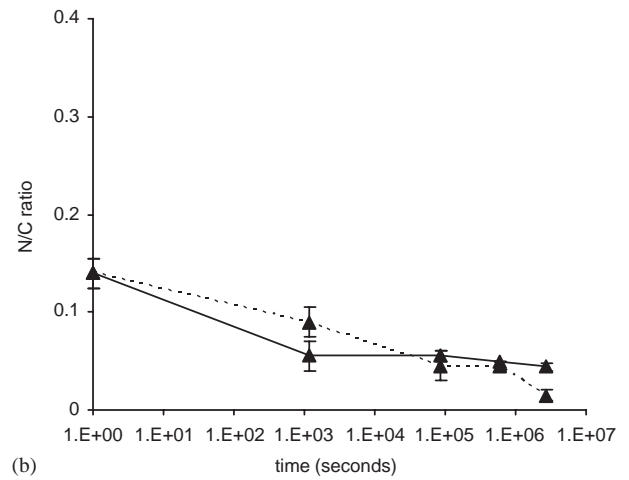
Fig. 3. Elemental ratios of N₂ plasma-treated PDMS as a function of time; (a) O/C; (b) N/C; and (c) Si/C. (—) Storage in PBS; and (---) storage in air. Mean ± standard deviation, n = 3.

3.1.2. O₂ and Ar plasma treatment

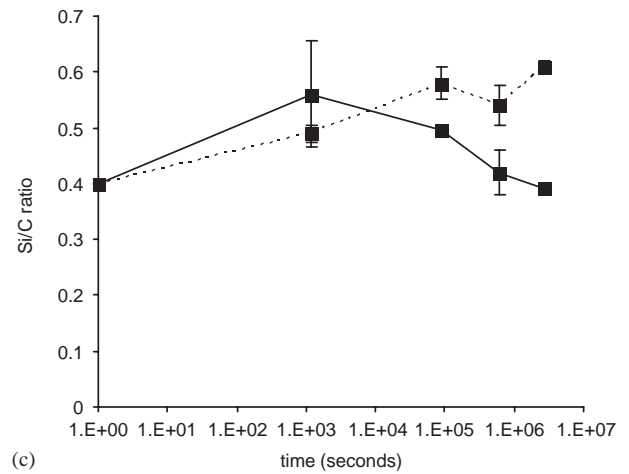
In the case of O₂ and Ar treatment, an increase in the intensity of the O-1s and Si-2p peaks was observed and



(a)



(b)



(c)

Fig. 4. Elemental ratios of NH₃ plasma-treated PDMS as a function of time; (a) O/C; (b) N/C; and (c) Si/C. (—) Storage in PBS; and (---) storage in air. Mean ± standard deviation, n = 3.

is concomitant with a decrease in the relative intensity of C-1s (Figs. 1 and 2). The C-1s envelope for O₂-treated PDMS could be deconvoluted into four components

Table 1
Integrated peak areas of deconvoluted high-resolution C-1s XPS spectral peaks relative to siloxane carbon in untreated PDMS (%)

Treatment	284.7 eV	286.5 (286) eV	287.1 eV	288 (288.2) eV	289 (289.2) eV
<i>Untreated</i>	100	—	—	—	—
1 month in air	100	—	—	—	—
1 month in PBS	93.4	6.6	—	—	—
<i>O₂ treated</i>	75.3	19	—	4.3	1.4
1 month in air	90	10	—	—	—
1 month in PBS	72.4	17.3	—	7.3	3
<i>Ar treated</i>	67.2	24	—	7.3	1.5
1 month in air	83.1	10.8	—	4.1	2.0
1 month in PBS	64.6	22.1	—	8.7	4.6
<i>N₂ treated</i>	50	16.1	13.8	11.6	8.5
1 month in air	69.7	11.4	7.8	6.9	4.2
1 month in PBS	66.7	11.6	11.6	6.5	3.6
<i>NH₃ treated</i>	56.9	27.5	8.6	4.8	2.4
1 month in air	67.4	19.6	5	6	2
1 month in PBS	70	16.5	6	5.5	2

Binding energies in parentheses refer to N₂- and NH₃-treated surfaces.

Table 2
Integrated peak areas of deconvoluted high-resolution Si-2p, O-1s and N-1s XPS spectral peaks relative to untreated O-1s (%)

Treatment	Si-2p			O-1s		N-1s		
	102.4 eV	103.6 eV	104.5 eV	532.4 eV	533.2 eV	399 eV	400 eV	401.2 eV
<i>Untreated</i>	91.5	8.5	—	100	—	—	—	—
1 month in air	91.5	8.5	—	100	—	—	—	—
1 month in PBS	82.9	17.1	—	100	—	—	—	—
<i>O₂ treated</i>	23.8	54.5	21.7	74.3	25.7	—	—	—
1 month in air	39.6	46.7	14.3	65	35	—	—	—
1 month in PBS	82.3	17.7	—	70	30	—	—	—
<i>Ar treated</i>	12	46.7	41.3	12.5	87.5	—	—	—
1 month in air	42.7	51.9	5.4	57.7	42.2	—	—	—
1 month in PBS	76.3	23.7	—	50	50	—	—	—
<i>N₂ treated</i>	35	65	—	66.2	33.8	20.8	52	27.2
1 month in air	73.7	26.3	—	89	11	16.5	53.9	16.5
1 month in PBS	76.5	23.5	—	44	56	34	51.3	14.7
<i>NH₃ treated</i>	65.7	34.3	—	79	21	30.4	56.9	12.8
1 month in air	75	25	—	75	25	—	100	0
1 month in PBS	79.1	20.9	—	77	23	16.9	69.4	13.7

(Table 1). The peak located at 284.7 eV is again associated with (C–Si–O–Si) bonds. The high binding energy shoulders identified at 286.5, 288 and 289 eV were assigned to carbon bound to oxygen as –C–O–, –C=O– and –COO– groups, respectively. The FWHM of the Si-2p peak increased from 1.8 to 2.9 eV and shifted from 102.6 to 103.6 eV suggesting an increase in the number of silica-containing moieties (Table 2). The Si-2p peak envelope was resolved into three species located at 102.4, 103.6 and 104.5 eV. The

main peak identified at 103.6 eV was associated with SiO₂ moieties and it is suggested that the peak at 104.5 eV was due to silicon in other multiple oxygen bonds including SiO₃ and SiO–OH–SiO. Similar spectra were observed after Ar treatment.

Ageing of O₂- and Ar-treated materials in PBS for periods of up to 1 month demonstrated an interaction with their ageing environment causing further chemical changes as a function of time, *t*, Figs. 1 and 2. Moreover, the reaction kinetics are different for each

treatment as shown by changes in the elemental ratios, O/C, and Si/C. In these figures, it can be seen that there is a decrease in both the Si/C and O/C ratios, most notably in the case of Ar treatment, Fig. 2. Ageing of O₂- and Ar-treated samples in air also resulted in a decrease in both the O/C and Si/C ratio but to a lesser extent than that found in PBS.

Further insight into the actual chemical reactions associated with the aged specimens can be gained by examining the deconvoluted high-resolution C-1s, Si-2p and O-1s spectra. The C-1s spectra (FWHM 2 eV) for both O₂- and Ar-treated PDMS aged in PBS for 1 month remained symmetrical and could be deconvoluted into four components with intensities and assignments similar to those obtained immediately after processing. In contrast, a decrease in the intensities of the C-1s components is observed after 1 month storage in air, most notably with O₂-treated PDMS. The Si-2p spectra for both O₂- and Ar-treated surfaces aged in PBS were found to be similar in that their peak positions shifted to a lower binding energy (102.7 eV) and the FWHM decreased from 3.0 to 1.9 eV. Consequently, their respective spectra could only be deconvoluted into two components with similar intensities to those assigned for the untreated material (Table 2). The corresponding Si-2p for air-stored O₂- and Ar-treated samples (FWHM 2.5 eV) is similar to that observed immediately after processing and can be deconvoluted into three components, the lower binding energy component (102.4 eV) increasing in intensity (Table 2). The O-1s peak (FWHM 2.1 eV) chemically shifted from 533.1 to 532.7 eV in both cases and the relative intensity of the 533.2 eV component decreased with respect to the 532.4 eV component.

3.2. N₂ and NH₃ plasma treatment

The incorporation of nitrogen onto the surface of PDMS following N₂ plasma treatment is evident (Fig. 3) and is concomitant with a reduction in the intensities of the O-1s and Si-2p peaks, whereas the intensity of the C-1s peak is essentially unchanged. A similar picture emerged after NH₃ treatment but to a lesser extent, Fig. 4. The C-1s peak (FWHM 3 eV) associated with N₂ treatment could be deconvoluted into a maximum of five peaks. The higher binding energy components are likely to represent carbon bound to nitrogen, since nitrogen atoms are incorporated during plasma treatment. A peak identified at 286 eV was consistent with the formation of $-\overset{\cdot}{\text{C}}-\text{N}-$ representative of amine groups in the form of $-\overset{\cdot}{\text{C}}-\text{NH}_2$ or $\overset{\cdot}{\text{C}}-\text{NHR}-$ whereas the component identified at 287.1 eV could represent $\overset{\cdot}{\text{C}}=\text{N}-$ or $-\text{N}-\overset{\cdot}{\text{C}}-\text{N}-$ type functionalities. The peaks located at 288.2 and 289.2 eV are thought to be representative of groups containing both oxygen and nitrogen. The peak at 288.2 eV could be indicative of

either $\text{R}-\overset{\cdot}{\text{C}}\text{O}-\text{NHR}$ or $\text{R}-\overset{\cdot}{\text{C}}\text{O}-\text{NH}_2$ -type functionalities rather than $-\overset{\cdot}{\text{C}}=\text{O}-$ considering the low uptake of oxygen observed immediately after processing. The peak at 289.2 eV could also represent either $\text{RNH}-\overset{\cdot}{\text{C}}\text{O}-\text{NHR}$ or $\text{N}-\overset{\cdot}{\text{C}}=\text{O}-\text{O}$. The C-1s spectrum for NH₃ treatment could also be resolved into five components with similar assignments but different intensities (Table 1).

The Si-2p peak (FWHM 2.6 eV) associated with N₂ treatment could be deconvoluted into two components (Table 2). The high binding energy shoulder (103.6 eV) increased in intensity suggesting that either SiO₂ or Si-N moieties were forming. The Si-2p could also be curve fitted into two components in the case of NH₃ treatment with similar assignments but different intensities (Table 2). In both cases, the O-1s spectra (FWHM 2.6 eV) chemically shifted from 532 to 533.6 eV, and could be deconvoluted into two species. The N-1s spectrum (FWHM 3.3 eV) associated with both N₂ and NH₃ treatment could be curve fitted into three peaks verifying that nitrogen-containing species had formed (Table 2). The low binding energy component (399 eV) was associated with $-\overset{\cdot}{\text{C}}-\overset{\cdot}{\text{N}}-$ groups whereas the higher binding energy components at 400 and 401.2 eV were representative of $-\overset{\cdot}{\text{C}}=\overset{\cdot}{\text{N}}-$ and $-\text{HNCO}-$, respectively.

The effect of ageing time on the elemental ratios of N₂- and NH₃-treated PDMS aged in PBS is shown in Figs. 3 and 4, respectively. With regard to N₂-treated surfaces, ageing in PBS resulted in a reduction in the N/C ratio which is paralleled by an increase in both the O/C and Si/C ratios, Fig. 3. NH₃-treated surfaces stored under similar conditions resulted in a reduction in both N/C and Si/C and an increase in O/C, Fig. 4. A similar pattern emerged following storage in air with similar reaction kinetics. Further insight into the actual chemical reactions associated with aged specimens can be provided by deconvoluted high-resolution C-1s, Si-2p and O-1s spectra (Tables 1 and 2). With regard to the C-1s spectrum (FWHM 2.4 eV), this peak became less pronounced in the high binding energy region of the spectrum for both treatments but most notably in the case of N₂ treatment. Also, the intensity of the 286 and 287.1 eV peaks, indicative of $-\overset{\cdot}{\text{C}}-\text{N}-$ and $-\overset{\cdot}{\text{C}}=\text{N}-$, respectively, reduced in intensity (Table 2). A similar picture emerged after storage in air. For both treatments, the Si-2p peak (FWHM 2.1 eV) became chemically shifted to 102.5 eV after storage in both PBS and air, the high binding energy component significantly reducing in intensity (Table 2). With regard to the O-1s spectrum (FWHM 2.4 eV), this peak was chemically shifted to 532.6 eV in both cases. The N-1s spectra obtained from N₂-treated specimens aged in PBS and air for 1 month could be deconvoluted into three components and their FWHMs were reduced in size to 2.5 and 2.2 eV, respectively. Furthermore, a reduction in the

peak at 401.2 eV was observed after storage and in the case of air storage, a reduction in the relative ratio of $C-N : C=N$ peaks occurred. A similar pattern was observed for the NH_3 -treated samples aged under similar conditions (Table 2).

3.3. Microscopy

Optical microscopy demonstrated plasma-induced cracking in the absence of a conductive coating (Fig. 5). A number of cracks can be observed which



Fig. 5. Typical optical micrograph of Ar plasma-treated PDMS showing curvy cracks.

are either ‘curvy’ or ‘orthogonal’ in appearance. In the case of N_2 - and NH_3 -treated PDMS, less surface cracking was observed.

The surface topography of untreated and plasma-treated specimens was also examined using AFM operated in ‘tapping’ mode. A typical AFM micrograph of Ar-treated PDMS is shown in Fig. 6. It can be seen that mild etching of the surface has occurred, producing surfaces that were more dimpled or pitted than the virgin surface. RMS roughness values for O_2 and Ar treatment were found to be approximately twice that of the untreated surface (Table 3). In the case of N_2 and NH_3 treatments, a fine globular texture was observed which wiped out the original parent polymer sub-microstructural features, the RMS roughness in both cases being comparable to untreated PDMS (Table 3).

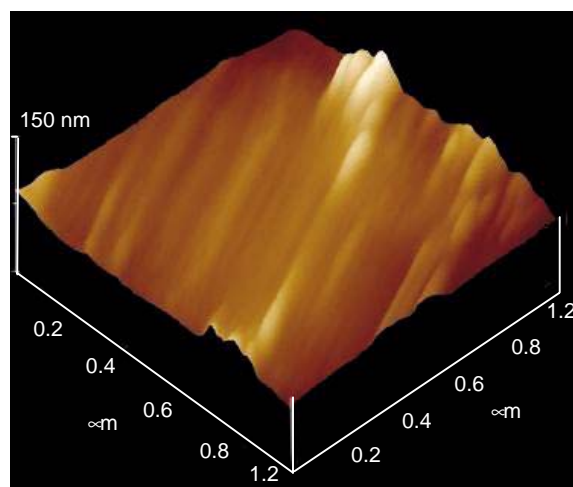
3.4. Wettability measurements

Contact angles were measured for virgin, plasma-treated and aged specimens up to 1 month using the Wilhelmy plate method in PBS. Untreated surfaces exhibited a hydrophobic nature characterised by relatively high values of advancing angle, $\theta_A = 103^\circ$, and

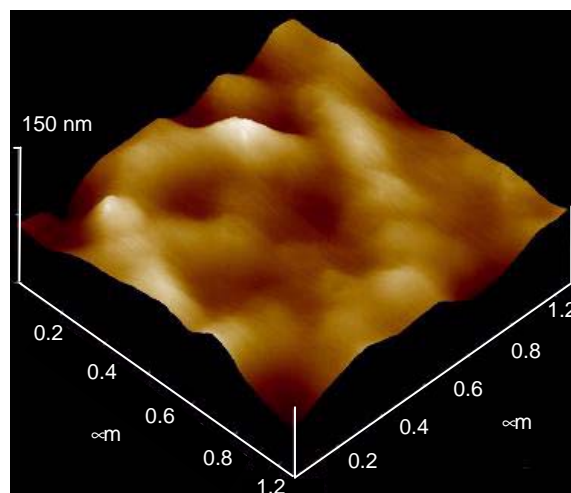
Table 3
RMS roughness and surface area ratios (a_r) for untreated and plasma-treated PDMS calculated from $1 \times 1 \mu m^2$ plots

Treatment	RMS roughness (nm)	Surface area ratio, a_r
Untreated	7 ± 1.6	1.05 ± 0.01
O_2 treated	14 ± 4.6	1.18 ± 0.04
Ar treated	13 ± 2.0	1.15 ± 0.02
N_2 treated	8 ± 3.0	1.13 ± 0.06
NH_3 treated	8 ± 2.1	1.12 ± 0.06

Mean \pm standard deviation, $n \geq 9$.



(a)



(b)

Fig. 6. AFM micrographs of (a) untreated; and (b) Ar plasma-treated PDMS, scan angle $\phi = 30^\circ$.

receding angle, $\theta_R = 70^\circ$, Table 4. All plasma treatments were effective in rendering the silicone rubber more hydrophilic, characterised by a reduction in the values of both θ_A and θ_R ; after treatment, θ_A values were in the range 46–73° and θ_R in the range 31–39° consistent with the incorporation of polar groups. Consequently, contact angle hysteresis $\Delta\theta$, measured on O₂, Ar and

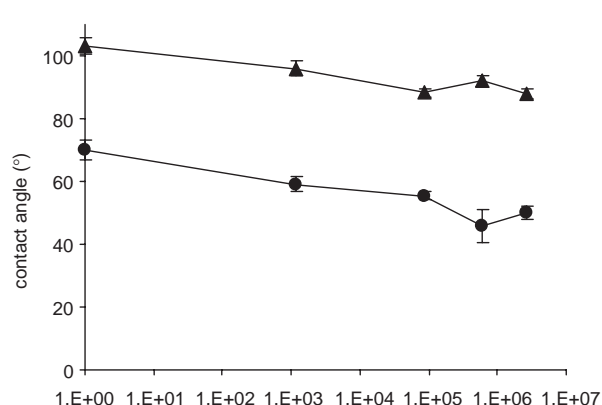
N₂ plasma-treated surfaces reduced from 34° (untreated PDMS) to values in the 12–20° range. However, $\Delta\theta$ for NH₃ plasma-treated surfaces remained high (34°).

DCA measurements also provided useful information regarding the wettability of aged specimens as a function of time, t , Fig. 7. Ageing in PBS induced a small increase in wettability of untreated PDMS surfaces which was

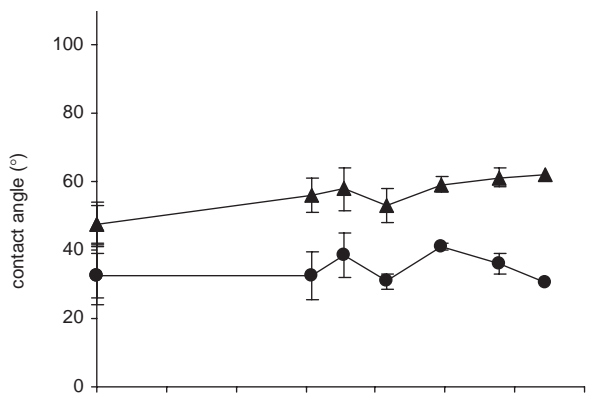
Table 4

Advancing and receding contact angle measurements in degrees for the untreated PDMS, immediately after gas plasma treatment, following storage in air for 1 month and following storage in PBS for 1 month

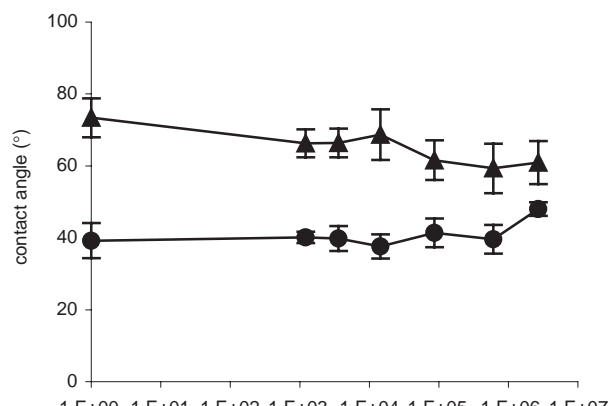
Treatment	Immediately after treatment		After ageing for 1 month in air		After ageing for 1 month in PBS	
	θ_A (deg)	θ_R (deg)	θ_A (deg)	θ_R (deg)	θ_A (deg)	θ_R (deg)
Untreated	103.0 ± 2.7	70.0 ± 3.3	101.9 ± 2.7	64.9 ± 3.2	87.8 ± 1.5	50.0 ± 1.9
O ₂	47.5 ± 6.6	32.7 ± 7.9	101.9 ± 2.7	64.9 ± 3.2	62.1 ± 2.7	30.3 ± 3.1
Ar	46.0 ± 5.6	33.1 ± 6.3	94.7 ± 2.3	48.2 ± 3.8	66.2 ± 4.3	43.4 ± 4.0
N ₂	58.1 ± 3.1	31.8 ± 7.8	97.3 ± 4.1	97.3 ± 4.1	74.5 ± 1.5	36.8 ± 6.5
NH ₃	73.4 ± 5.4	39.2 ± 4.9	92.3 ± 2.5	92.3 ± 2.5	60.9 ± 6.0	48.0 ± 1.9



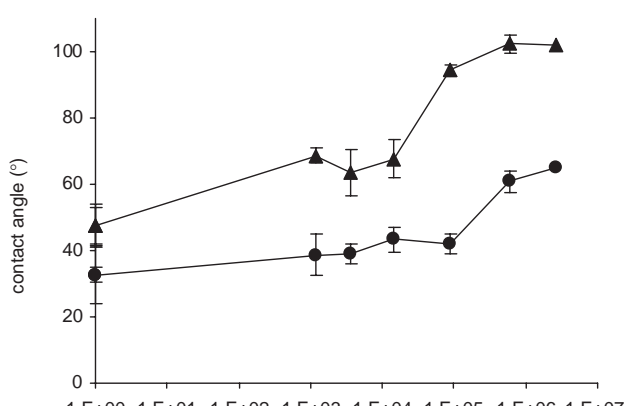
(a) time (seconds)



(b) time (seconds)



(c) time (seconds)



(d) time (seconds)

Fig. 7. Contact angles as a function of time of PDMS: (a) untreated; (b) O₂ plasma treated following ageing in PBS; (c) NH₃ plasma treated following ageing in PBS; and (d) O₂ plasma treated following ageing in air. (▲) Advancing angle (θ_A); and (●) receding angle (θ_R). Mean ± standard deviation, $n = 6$.

characterised by a decrease in both θ_A ($103\text{--}88^\circ$) and θ_R ($70\text{--}50^\circ$). However, contact angle hysteresis $\Delta\theta$, remained essentially unchanged, Fig. 7(a). On the other hand, storage of plasma-treated specimens in PBS resulted in a slight increase in θ_A^{PBS} (Fig. 7b), with the exception of NH_3 treatment, Fig. 7(c). The values for θ_R , however, were essentially unaffected after prolonged storage in PBS. Ageing in air resulted in almost complete recovery of θ_A and an increase in θ_R , most notably after O_2 treatment, Fig. 7(d). Consequently, $\Delta\theta$ values for air-stored samples remained high.

3.5. PTT analysis

The clotting times of untreated and plasma-treated surfaces fell within the range defined by the controls, Fig. 8. Contact with untreated PDMS resulted in a decrease in clotting time from 193 to 145 s ($p = 0.002$) compared to non-contacted PPP. With respect to the untreated material, treatment in O_2 and Ar resulted in a further reduction in clotting time to 106 and 127 s, respectively, indicating a reduction in haemocompatibility for the O_2 -treated sample ($p < 0.05$). Plasma treatment in N_2 and NH_3 resulted in an increase in clotting time to 186 and 181 s, respectively, indicating a significant improvement in haemocompatibility ($p = 0.026$ and 0.068 , respectively (p values without the Bonferroni correction are 0.003 and 0.01 , respectively)). N_2 -treated PDMS, therefore, exhibited the longest clotting time and represents the smallest degree of activation. Conversely, plasma treatment with O_2 exhibited the highest degree of activation.

Whilst it is common practice to interpret a longer coagulation time of a PTT assay as being indicative of reduced contact activation, it is possible that this may arise from the inhibition, destruction or removal of coagulation factors or cofactors as a result of the contact of the PPP with the biomaterial. To test for

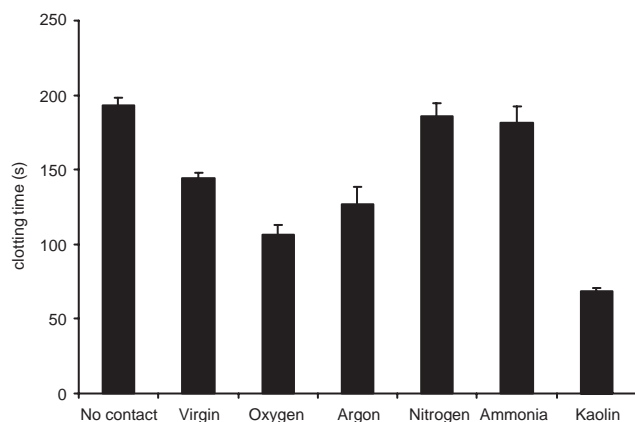


Fig. 8. Effect of plasma treatment on the activation of the intrinsic coagulation system by PTT analysis, Mean \pm SEM, $n = 4$.

this possibility, PPP that had been contacted with NH_3 -treated PDMS was hyper-activated with a mixture of dispersed kaolin and synthetic phospholipids, then analysed by PTT. These were compared with hyper-activated PPP from the same pool that had received no contact. The results showed that there was no difference in coagulation time (33.0 ± 3.0 s for NH_3 -treated PDMS; 33.5 ± 3.5 s for control PPP), establishing that the longer coagulation times were due to low contact activation.

Although a calibration curve for the PTT analysis was not specifically generated during this set of experiments, donors from the same plasma pool were used to generate such a graph using concentrations of kaolin in the range 2–1000 mg/ml. Consequently, as demonstrated previously [32], one can estimate that the coagulation activating powers of the treated PDMS relative to untreated PDMS range from approximately 0.06 for N_2 -treated PDMS to 12.8 for O_2 -treated PDMS.

4. Discussion

The objectives of the present research were to determine the chemical and morphological surface modifications of PDMS induced by four plasma treatments and after ageing in either PBS or air and estimate the influence of these modifications on haemocompatibility. In the present study, several complementary techniques have been used to investigate the consequences of plasma treatment of PDMS surfaces. From the results obtained, it has emerged that the surface properties (morphology, chemistry and wettability) of PDMS can be modified by plasma treatment in O_2 , Ar, N_2 and NH_3 gas atmospheres. The chemical changes which were found to occur fall into two categories: (i) side group modifications and (ii) chain scission. In addition, there is evidence that ageing involved ongoing changes of surface chemistry which fall into two further categories: (iii) post-treatment chemical reactions and (iv) surface relaxation. It is important to analyse the specific surface modifications that have been created by a particular plasma system since comparison between different systems is not valid. If these surface modifications are to be used practically for medical devices, the analysis of aged samples is essential. This study clearly demonstrated that surface modification of silicone rubber by gas plasmas and ageing environments influenced the haemocompatibility of the material.

The plasma treatments resulted in increases of surface rugosity on the sub-micron scale, leading to enhancements of surface areas by about 5–11% for all treated surfaces. Mild etching was attributed to the removal of $-\text{CH}_3$ groups in the case of O_2 and Ar treatment and Si–O groups in the case of N_2 and NH_3 treatments and

all plasma treatments resulted in the exposure of underlying silica filler. Microcracks were frequently observed after O₂ and Ar treatments and were probably due to an increase in shrinkage stresses generated in the brittle silica layer, the average crack spacing typically being 1 μm.

The principal chemical change induced by O₂ and Ar plasma treatment was the removal of pendant methyl groups by the rupture of the Si–C bond. In contrast, N₂ and NH₃ treatments primarily attacked the Si–O bond which is unexpected since Si–O is more stable than Si–C. Another chemical change that occurred during plasma treatment was the incorporation of new functional groups by reaction of the activated surface with species present in the plasma. In the case of O₂ treatment, methyl side groups were substituted by more polar entities such as hydroxyl, carbonyl and carboxylic groups through reaction with O, OH and O₂ plasma species [33]. In this study, exposure to air during sample transfer resulted in all samples experiencing physisorption and chemisorption of atmospheric oxygen and water vapour which also lead to increased functionality, most notably after Ar treatment. In addition, surface oxidation may have been augmented by plasma attack of the glass reactor, producing oxygen-containing species in the cell.

In all cases, plasma treatment resulted in an increase in wettability of materials in PBS as shown by a decrease in both θ_A and θ_R . The decrease in θ_A was attributed to an increase in the surface concentration of polar groups, i.e. replacement of methyl groups by a silica layer in the case of O₂ and Ar treatment and by nitrogen-containing groups in the case of N₂ and NH₃ treatment.

Ageing of plasma-treated polymers has been investigated by several workers and the chemical changes are often found to be either partially or totally reversible as the time from plasma treatment increases [9]. It has been established that two principal mechanisms occur, (i) post-treatment chemical reactions and (ii) surface relaxation [4,9]. Thus, when a material is to be used in a particular application, it is necessary to know the nature and kinetics of potential processes. In the present work, plasma-treated specimens were aged in either air or PBS and subsequent changes in wettability and chemistry were determined.

The surface elemental composition of untreated PDMS remained essentially unchanged following prolonged storage in PBS. Although a slight increase in wettability was observed, the measured contact angle hysteresis remained essentially unchanged. In the case of plasma-treated materials, two post-reactions were observed during ageing (a) removal of unstable nitrogen-containing groups in the case of N₂ and NH₃ treatment [16,17,28] and (b) removal of silica-like groups, most notably with O₂- and Ar-treated speci-

mens, resulting in a reduction in wettability. In the case of Ar and O₂ treatment, the reduction in oxygen concentration could be explained by the extraction of silica-like groups through the cracked-treated layer by dissolution processes. The remaining oxygen species present in the surface were indicative of stable carbon functionalities introduced into the surface following plasma exposure. Alternatively, the loss of silica may also have occurred as a result of the formation of a weak boundary layer [17]. A number of studies have shown that there is a maximum level of plasma treatment at which surfaces are stable to washing with a solvent [28,34]. Above this level, a measurable amount of modified material is removed by washing. In this study, the ‘saturation’ time was defined as the time at which no more oxygen is incorporated with further treatment and was previously calculated to be 30s for PE [17]. Consequently, the treatment time used for PDMS appears to be greater than the saturation time resulting in the formation of a weak boundary layer.

Storage in air resulted in hydrophobic recovery attributed to relaxation in the surface. Despite XPS measurements indicating that a large fraction of polar groups was still present in the modified region of air-stored samples, contact angle measurements suggested otherwise. This apparent anomaly is explained by the relative surface sensitivity of the two techniques. In the former technique, elemental information was obtained from a depth of about 3 nm. However, in the latter case, surface sensitivity is of the order of 1 nm and suggests that a depletion in surface concentration of polar groups occurred following storage in air. Furthermore, XPS measurements indicated that the decrease in oxygen concentration observed was attributed to loss of carbon species bound to oxygen rather than silicon to oxygen since the former functionalities are likely to be more mobile. The loss of ‘silica-like’ species occurred at a lower rate than that observed in PBS since most of them originate from exposed filler and, therefore, persist in the surface longer, enabling unmodified PDMS to migrate over the filler surface.

The interpretation of wettability data on chemically heterogeneous and topographically rough surfaces requires specific analysis [35]. A theoretical guide to the wettability of heterogeneous surfaces was introduced initially by Cassie [36] and later modified by Israelachvili and Gee [37]. To summarise these hypotheses, one should consider a surface that is comprised of two regions with distinct chemistry, one being relatively less wettable and the other more wettable by the working fluid of interest. The surface concentrations of these two regions are designated X^L and X^M for the less- and more-wettable fractions, respectively, with $X^L + X^M = 1$. The contact angle for idealised surfaces is expected to vary between the extreme values, θ_Y^L (corresponding to

$X^L = 1$) and θ_Y^M (corresponding to $X^M = 1$). In these models, the dimensions of the two intermixed chemical regions are on the molecular scale, and hence no hysteresis arises. In effect, surfaces with intermediate values of X^L and X^M are conceived as having an ‘averaged’ chemical character on a macroscopic scale, and hence exhibit ideal Young contact angles with values between θ_Y^L and θ_Y^M . Heterogeneous surfaces where the dimensions of the intermixed less- and more-wettable fractions are microscopic or larger would be expected to exhibit the same trend of wettability as a function of X^M as for the idealised surface, but with hysteresis, $\Delta\theta = \theta_A - \theta_R$, superimposed. Johnson and Dettre [38] have investigated the extent of such hysteresis for hypothetical surfaces with particular geometries of the intermixed regions.

In the present work, with PBS as the working fluid, the idealised surface of virgin PDMS is smooth and chemically homogeneous with $X^L = 1$. Plasma treatments can induce finite concentrations, X^M depending on the number and nature of polar groups introduced to the surface, in addition to some roughness. Estimates of X^L and X^M for PDMS surfaces have been obtained on the basis of deconvoluted peak areas in the Si-2p spectra of XPS measurements. Si-2p was chosen since the envelope incorporates peaks chemically shifted with respect to that for siloxane (C–Si–O–Si) due to bonds formed between Si and O. The wettability of idealised virgin material is regarded as arising from a smooth surface saturated with methyl groups. Plasma modification may introduce groups which are more polar than this reference, e.g. C–OH and C–N. These groups are thought to arise due to modifications of side groups in the initial material. For measurements of contact angles in PBS, X^M is taken to be the sum of the areas of the individual deconvoluted peaks due to the groups more polar than CH₃ divided by the (unit) area of the Si-2p convolution. For measurements in PBS, θ_Y^L and θ_Y^M were taken to be 80° and 20°, respectively, corresponding to idealised virgin surfaces and saturated polar surfaces, respectively.

The variation of advancing and receding contact angles measured in PBS is plotted against the surface concentration of the more wettable fractions, X^M in Fig. 9(a). As an aid to discussion, the variation of θ_Y for idealised surfaces is also plotted as a function of X^M . It is presumed that the hysteresis associated with virgin materials arises due to the modest surface roughness present and to reorientation of the more wettable silicate backbone. For O₂- and Ar-plasma treatment, a large fraction of polar side-groups is introduced combined with additional light etching. These changes significantly reduce both θ_A and θ_R and cause the hysteresis to diminish, tending towards the behaviour of an idealised wetting surface with Young angle equal to θ_Y^M and $\Delta\theta = 0$. For the other two treatments, N₂ and NH₃

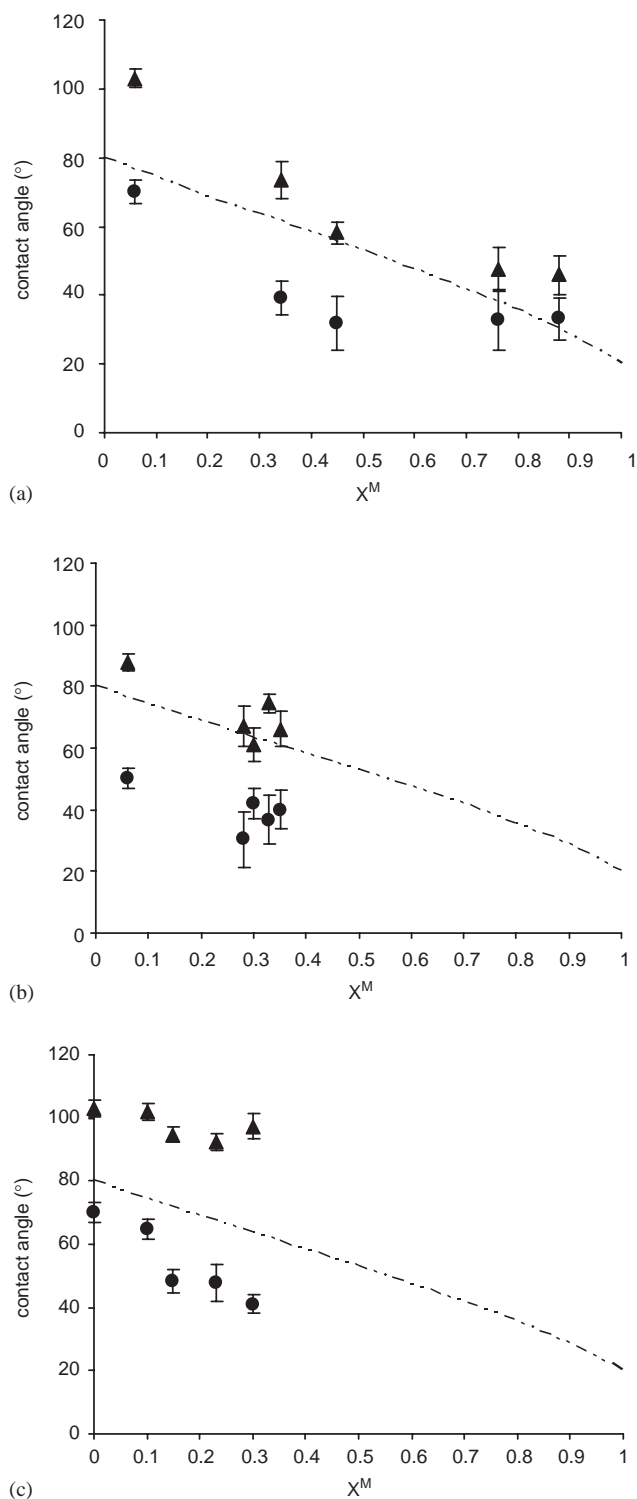


Fig. 9. Contact angle hysteresis as a function of X^M (a) immediately after processing; (b) following 1 month ageing in PBS; and (c) following 1 month storage in air (wetting fluid, PBS). (\blacktriangle) Advancing angle (θ_A); and (\bullet) receding angle (θ_R). Mean \pm standard deviation, $n = 6$.

plasma treatments introduced lower concentrations, X^M , of polar groups than for O₂ treatment, and the level of etching was less pronounced, but within the

same range. This results in less reduction in θ_A and θ_R and less reduction in hysteresis. These trends in the variation of $\Delta\theta$ with X^M are consistent with the predictions of Johnson and Dettre [38] for hypothetical heterogeneous surfaces.

In the present context, we anticipate that storage in either PBS or air can lead to time-dependent changes in addition to those caused by the initial plasma treatment. Fig. 9(b) shows the variation of θ_A and θ_R for materials stored in PBS for 1 month when examined with PBS as the wetting fluid. Estimates of X^L and X^M for aged surfaces have been obtained on the basis of deconvoluted peak areas in the C-1s spectra of XPS measurements. C-1s was chosen in preference to Si-2p since the outer layer of silica is lost after storage in PBS exposing an underlying layer of oxidised-carbon groups. A comparison of Figs. 9(a) and (b) emphasises that the effect of storage in PBS is to reduce the wettability (increasing θ_A), particularly for O₂ and Ar plasma-treated materials. The principal mechanism operating in this case is a chemical reaction with the storage medium resulting in the destruction of the outer silica layer, thereby reducing X^M .

When this method of analysing variations in wettability is applied to air-stored samples, it is seen that significant recovery of the material towards its untreated state occurs as shown by an increase in θ_A and decrease in X^M , Fig. 9(c). The reduction in the number of more wettable groups can be attributed to the diffusion of unmodified chain segments outwards from the bulk to the surface.

The PTT analysis indicated that the plasma treatments induced a considerable change in the propensity for fXII to be activated during blood contact compared with standard PDMS. It is generally understood that almost all commonly used medical-grade biomaterials induce activation, at least to some degree, of the processes that lead to clot formation [26,39], one aspect of this being activation of the intrinsic coagulation cascade. It is no surprise, therefore, to observe that unmodified PDMS caused a significant reduction in clotting time compared to unactivated PPP. The coagulation cascade is a complex system of plasma proteins which becomes sequentially activated (cleaved), with amplification occurring throughout the reaction sequence. Thus, differential activation of the contact phase system has been demonstrated to lead to clotting times which are exponentially related to the concentration of the activating agent [32]. Consequently, small differences in the clotting times can, therefore, hide large differences in the true level of fXII activation. This leads to the extrapolation that N₂-treated PDMS activates the coagulation system to approximately only 0.06 times that of unactivated PDMS.

The trend of fXII activation potential of the different plasma gas treatments is the same as that observed for

treatment of a polyetherurethane (PEU) in another study using the same plasma system [32]. Interestingly, unmodified PEU was demonstrated to be the most thrombogenic material in the PEU series, whereas Ar and O₂ treatments rendered PDMS less haemocompatible, reflecting the experience of nitrogen and oxygen treatments in other studies [39]. These results, therefore, indicate that there is an atomic basis for the activation of fXII, and it is unlikely that the coagulation activation reaction is controlled merely by generic parameters such as surface charge or surface energy. Indeed, continuing observations that hydrophobic surfaces are inefficient contact activators [40] appear to be challenged by this study. It is often observed that attempts to improve biomaterial thrombogenicity often fail, with indifferent results despite radical changes to the surface chemistry [20].

There are a few rules of thumb that have been established regarding the acceptability of certain surface chemical groups for the prevention of different blood compatibility-related phenomena. For example, it has been known for many years that increasing the water content in HEMA hydrogels leads to thrombogenic events [21] and although protein adsorption may be reduced in this scenario, it is likely to lead to an increase in complement activation [20], since hydroxyl groups are known complement activators. This is apparently paradoxical, since one might expect hydrophilic surfaces to present an environment more similar to an aqueous milieu, resulting in a reduction in conformational and therefore activating perturbations to an adsorbed protein layer.

The methylation of surfaces has been shown to reduce the activation of fXII [41], and the ratios of O:C at the surface has also been implicated as an important factor in this respect: slowly increasing the O/C ratio in collagen by exposure to UV was demonstrated to lengthen plasma clotting time [42] and surface treatments of polystyrene with high surface O concentrations caused reduced levels of contact activation [39]. These reports are opposite to the findings in this study. In the study of plasma-treated PEU [32], the ratio of O:N was suggested as a factor, the activating surfaces PEU-O₂ and PEU-Ar registering 7.1 and 7.7, and non-activating surfaces PEU-N₂ and PEU-NH₃ registering 0.8 and 1.3. However, in the current study the equivalent figures of surface O:N for PDMS-N₂ and PDMS-NH₃ was 1.1 and 3.5, suggesting that the absolute ratio is of little relevance.

Undoubtedly, the structural requirements for adsorbed protein activation will be a combination of surface atomic concentration, their geometry and microheterogeneity. It is possible that fXII becomes activated in a process that is not entirely as a result of a formal adsorption step, as proposed by Vogler [40].

5. Conclusions

Plasma treatment of PDMS caused changes in surface chemistry combined with mild etching, leading to increased wettability. The chemical changes induced were side group modification and chain scission, the extent of which varied with the plasma gas. All plasma treatments etched, to varying degrees, the PDMS surface exposing some of the filler and produced some additional 'silica-like' material. In addition, a number of microcracks were observed as a consequence of the thin, brittle layer of silica. The stability of plasma-treated surfaces to ageing in PBS resulted in the destruction of the silica layer following O₂ and Ar plasmas treatment and removal of nitrogen-containing moieties following N₂ and NH₃ treatment. The hysteretic wetting behaviour of plasma-treated and aged specimens was correlated semi-quantitatively with the surface concentrations of more wettable groups, and was shown to resemble the predictions of previously published theoretical models.

PDMS haemocompatibility was dramatically affected by plasma treatment, both N₂ and NH₃ treatments causing a highly significant reduction in fXII activation caused by incubation with the surfaces, that of NH₃ to a level almost indistinguishable from non-contacted PPP. Treatment of PDMS with both Ar and O₂ induced a decrease in haemocompatibility, leading to shorter clotting times.

Acknowledgements

The authors of this paper would like to thank Dr. Hans Griesser (CSIRO, Melbourne) for kindly providing use of high-resolution XPS facilities. The EPSRC is gratefully acknowledged for providing a PhD studentship for Darren Wilson and an Advanced Research Fellowship for Nicholas Rhodes. Parts of the research were performed as part of the Interdisciplinary Research Collaboration in Tissue Engineering for which funds were provided by the BBSRC, MRC and EPSRC.

References

- [1] Ross AH, Griffith CD, Anderson JR, Grieve DC. Thromboembolic complications with silicone elastomer subclavian catheters. *J Parenter Enter Nutr* 1982;6:61–3.
- [2] Dollery CM, Sullivan ID, Bauraind O, Bull C, Milla PJ. Thrombosis and embolism in long-term central venous access for parental nutrition. *Lancet* 1994;344:1043–5.
- [3] Morra M, Occhiello E, Garbassi F, Johnson D. On the ageing of oxygen plasma-treated polydimethylsiloxane surfaces. *J Colloid Interface Sci* 1990;137:11–24.
- [4] Owen MJ, Smith PJ. Plasma treatment of polydimethylsiloxane. *J Adhes Sci Technol* 1994;8:1063–75.
- [5] Stewart MT, Urban MW. ATR FT-IR characterization of the gas-plasma modified silicone-rubber surfaces. *Abstr Pap Am Chem Soc* 1988;196:71.
- [6] Gaboury S, Urban MW. Spectroscopic evidence for Si–H formation during microwave plasma modification of poly(dimethylsiloxane) elastomer surfaces. *Polym Commun* 1991;32:390–2.
- [7] Hall R, Westerdahl CAL, Devine AT, Bodnar MJ. Activated gas plasma surface treatment of polymers for adhesive bonding. *J Appl Polym Sci* 1969;13:2085–96.
- [8] Hollahan J, Carlson G. Hydroxylation of polymethylsiloxane surface by oxidizing plasmas. *J Appl Polym Sci* 1970;14:2499–508.
- [9] Triolo PM, Andrade JD. Surface modification and evaluation of some commonly used catheter materials. 1. Surface properties. *J Biomed Mater Res* 1983;17:129–47.
- [10] Feneberg P, Krekler U. Process for the production of hydrophilic surfaces on silicon elastomer articles. US Patent No. 3959105, 1976.
- [11] Fakes DW, Davies MC, Brown A, Newton JM. The surface-analysis of a plasma modified contact-lens surface by SSIMS. *Surf Interface Anal* 1988;13:233–6.
- [12] Everaert EP, Van der Mei HC, Devries J, Busscher HJ. Hydrophobic recovery of repeatedly plasma-treated silicone-rubber. 1. Storage in air. *J Adhes Sci Technol* 1995;9:1263–78.
- [13] Lai JY, Lin YY, Denq YL, Chen JK. Surface modification of silicone rubber by gas plasma treatment. *J Adhes Sci Technol* 1995;10:231–42.
- [14] Urban MW, Stewart MT. DMA and ATR FT-IR studies of gas plasma modified silicone elastomer surfaces. *J Appl Polym Sci* 1990;39:265–83.
- [15] Kuznetsov AY, Bagryansky VA, Petrov AK. The surface relaxation of glow discharge-treated silicone polymer. *J Appl Polym Sci* 1995;57:201–7.
- [16] Wilson DJ, Williams RL, Pond RC. Plasma modification of PTFE surfaces. Part I: surfaces immediately following plasma treatment. *Surf Interface Anal* 2001;31:385–96.
- [17] Wilson DJ, Williams RL, Pond RC. Plasma modification of PTFE surfaces. Part II: plasma-treated surfaces following storage in air or PBS. *Surf Interface Anal* 2001;31:397–408.
- [18] Lin YS, Hlady V, Janavota J. Adsorption of complement proteins on surfaces with a hydrophobicity gradient. *Biomaterials* 1992;13:497–504.
- [19] Wojciechowski PW, Brash JL. Fibrinogen and albumin adsorption from human blood plasma and from buffer onto chemically functionalized silica substrates. *Colloid Surf B* 1993;1:107–17.
- [20] Sefton MV, Sawyer A, Gorbet M, Black JP, Cheng E, Gemmell C, Pottinger-Cooper E. Does surface chemistry affect thrombogenicity of surface modified polymers? *J Biomed Mater Res* 2001;55:447–59.
- [21] Hoffman AS, Cohn D, Hanson SR, Harker LA, Horbett TA, Ratner BD, Reynolds LO. Application of radiation-grafted hydrogels as blood-contacting biomaterials. *Radiat Phys Chem* 1983;22:267–83.
- [22] Lyman DJ, Brash JL, Chaikin SW, Klein KG, Carini M. The effect of chemical structure and surface properties of synthetic polymers on the coagulation of blood. II. Protein and platelet interaction with polymer surfaces. *Trans Am Soc Artif Intern Organs* 1968;14:250–5.
- [23] Baier RE, Dutton RC. Initial events in interactions of blood with a foreign surface. *J Biomed Mater Res* 1969;3:191–206.
- [24] Baier RE. The role of surface energy in thrombogenesis. *Bull NY Acad Med* 1972;48:257–72.
- [25] Sawyer PN, Srinivasan S. The role of electrochemical surface properties in thrombosis at vascular interfaces: cumulative experience of studies in animal and man. *Bull NY Acad Med* 1972;48:235–56.

- [26] Ratner BD. The blood compatibility catastrophe. *J Biomed Mater Res* 1993;27:283–8.
- [27] Gorbet MB, Yeo EL, Sefton MV. Flow cytometric study of in vivo neutrophil activation by biomaterials. *J Biomed Mater Res* 1999;44:289–97.
- [28] Pringle SD, Joss VS, Jones C. Ammonia plasma treatment of PTFE under known plasma conditions. *Surf Interface Anal* 1996;24:821–9.
- [29] O’Kell S, Henshaw T, Farrow G, Aindow M, Jones C. Effects of low-power plasma treatment on polyethylene surfaces. *Surf Interface Anal* 1995;23:319–27.
- [30] Rhodes NP, Williams DF. Plasma recalcification as a measure of contact phase activation and heparin efficacy after contact with biomaterials. *Biomaterials* 1994;15:35–8.
- [31] Briggs D. Applications of XPS in polymer technology. In: Briggs D, Seah MP, editors. *Practical surface analysis, Auger and X-ray photoelectron spectroscopy*, vol. 1, 2nd ed. New York: Wiley; 1990. p. 436–83.
- [32] Wilson DJ, Rhodes NP, Williams RL. Surface modification of a segmented polyetherurethane using a low powered gas plasma and its influence on the activation of the coagulation system. *Biomaterials* 2003;24:5069–81.
- [33] Hansen RH, Pascale JV, Benedictis TD, Rentzepis PM. Effect of atomic oxygen on polymers. *J Polym Sci A* 1965;3:2205–14.
- [34] France RM, Short RD. Plasma treatment of polymers—effects of energy transfer from an argon plasma on the surface chemistry of poly(styrene), low density poly(ethylene), poly(propylene) and poly(ethylene terephthalate). *J Chem Soc Faraday Trans* 1997; 93:3173–8.
- [35] Wilson DJ, Pond RC, Williams RL. Wettability of chemically modified polymers: experiment and theory. *Interface Sci* 2000;8: 389–99.
- [36] Cassie ABD. Discuss. *Faraday Soc* 1952;57:5041.
- [37] Israelachvili JN, Gee ML. Contact angles on chemically heterogeneous surfaces. *Langmuir* 1989;5:288–9.
- [38] Johnson RE, Dettre RH. Wettability and contact angles. In: Matijevic E, editor. *Surface and colloid science*, vol. 2. New York: Wiley-Interscience; 1969. p. 85–153.
- [39] Grunkemeier JM, Tsai WB, Horbett TA. Hemocompatibility of treated polystyrene substrates: contact activation, platelet adhesion, and procoagulant activity of adherent platelets. *J Biomed Mater Res* 1998;41:657–70.
- [40] Vogler EA. Structure and reactivity of water at biomaterial surfaces. *Adv Colloid Interface Sci* 1998;74:69–117.
- [41] Tengvall P, Askendal A, Lundström I, Elwing H. Studies of surface activated coagulation: antisera binding onto methyl gradients on silicon incubated in human plasma in vitro. *Biomaterials* 1992;13:367–74.
- [42] Tyan Y-C, Liao J-D, Klausner R, Wu I-D, Weng C-C. Assessment and characterization of degradation effect for the varied degrees of ultra-violet radiation onto the collagen-bonded polypropylene non-woven fabric surfaces. *Biomaterials* 2002;23:65–76.